View metadata, citation and similar papers at core.ac.uk
brought to you by CORE
provided by Greenwich Academic Literature Archive

Systematic comparison of the functional physico-chemical characteristics and biocidal activity of microbial derived biosurfactants on blood-derived and breast cancer cells

Olufunke Akiyode[1], Daliya George[1], Giulia Getti[1], Joshua Boateng[1*]

[1]Faculty of Engineering and Science, University of Greenwich, Medway, Kent, UK ME4 4TB

*Correspondence: Dr Joshua Boateng (j.s.boateng@gre.ac.uk; joshboat40@gmail.com)

ABSTRACT

Hypothesis

The cytotoxicity of biosurfactants on cell membranes may be influenced by composition of their hydrophilic head and hydrophobic tails. It is hypothesised that they form mixed micelles which exert a detergent-like effect that disrupts the plasma membrane. The functional physico-chemical and biocidal characteristics of four biosurfactants were concurrently investigated to determine which of their structural characteristics may be tuned for greater efficacy.

Experiments

Rhamnolipid-95, rhamnolipid-90, surfactin and sophorolipid were characterised using FTIR, LC-MS, HPLC, surface tension and critical micelle concentration. Their biocidal activity against HEK 293, MCF-7 and THP-1 cell lines were investigated by MTT assay, using doxorubicin as cytotoxic control. Growth curves were established for all cell lines using trypan blue (TB) and MTT assays, corresponding doubling time (DT) and growth rate were obtained and compared.

Findings

HEK 293 cell-line had the highest growth rate amongst the three cell lines. For TB assay, growth of HEK 293 > THP-1 and for MTT, HEK 293 > MCF-7 while the DT was in the order of THP-1 > MCF-7 > HEK 293. Sophorolipid showed anti-proliferative activity comparable to doxorubicin on THP-1 > MCF-7 > HEK 293. THP-1 showed high sensitivity to sophorolipid with IC_{50} of 10.50, 25.58 and 6.78 (µg/ml) after 24, 48 and 72 hr respectively. However, sophorolipid was cytotoxic from 24-72 hr on HEK 293 cell lines with IC_{50} of 21.53, 40.57 and 27.53 µg/ml respectively. Although, doxorubicin showed higher anti-proliferative activity than all biosurfactants, it had poorer selectivity index for the same time durations compared to the biosurfactants. This indicates that biosurfactants were more effective for slowing the growth of the tested cancer cell lines and hence may be potential candidates for use in human cancer therapy. Physico-chemical characteristics of the biosurfactants suggest that their mechanism of action may be due to activity on the cell membrane.

Keywords: Biosurfactants, cancer chemotherapy, critical micelle concentration, cytotoxicity, HEK 293, MCF-7, rhamnolipid, sophorolipid, surfactin, THP-1.

1. INTRODUCTION

Surfactants are amphiphilic compounds that consist of a hydrophilic head and hydrophobic tail and have surface activity (Hu, 2010). The hydrophilic part can be a charged polar group (e.g. sulphate), a zwitterionic group (e.g. glycine) or uncharged polar group (e.g. poloxamers), whereas the hydrophobic part can be a non-polar group, comprising a single carbon chain or up to four alkyl chains (Tonova and Lazaravo, 2008). Based on the nature of their polar head group, surfactants can be classified as anionic, non-ionic, zwitterionic and cationic, (Holmberg *et al*., 2003; Pashley and Karaman, 2004; Rosen, 1978. They are synthesized from petrochemical sources such as sodium lauryl sulphate, polyoxyethylene glycol octylphenol ethers, phospholipids and alkyltrimethylammonium salts (Scarlat, 2015) and used in the formulation of detergents, personal care products and cleaning agents, (Scarlat, 2015) and this is possible through their surface active and interfacial properties.

Surfactants are also secreted by mammals (pulmonary surfactants), plants (lecithin), and microorganisms and these are referred to as biosurfactants to differentiate them from the chemically synthesised ones. Microbial biosurfactants (BSs) exist as low and high molecular weight compounds such as rhamnolipids, sophorolipids, surfactin, trehalose lipids and emulsan. They are further sub-divided into glycolipids (rhamnolipids, sophorolipids), lipopeptides, (surfactin) and polymeric BSs (emulsan). Due to their natural origins, BSs are recognised as non-toxic or of low toxicity, biodegradable and therefore potential alternatives to synthetic surfactants (Harshada, 2014). In addition, BSs are multifunctional compounds that also have biotechnological and biomedical applications. The BSs investigated in this study (rhamnolipids, surfactin and sophorolipids) were selected on the basis of their therapeutic and biophysical properties as well as their ready availability. Rhamnolipids and sophorolipids are members of the same glycolipid sub-class while surfactin is a macrolide lipoheptapeptide (Kakinuma *et al*., 1969) and are amongst the most widely characterised biosurfactants and also used in several applications.

Rhamnolipids are synthesised from *Pseudomonas aeruginosa* (Bergstrom *et al*., 1946) and exist as a family of congeners, some of which have isomers. The most prominent congeners are mono-rhamnolipids and di-rhamnolipids with molecular formulas Rha-C_{10}-C_{10} and Rha-Rha-C_{10}-C_{10} respectively (Figure 1). The structural units were further elucidated as being composed of two β-hydroxydecanoic acids linked through an ester bond to two rhamnose moieties via a 1,3 glycosidic linkage (Figure 1). The ratio of mono to di-rhamnolipids (Figure 1A & 1B) produced by bacteria depends on the carbon sources utilised during biosynthesis (Lotfabad *et al*., 2010). The di-rhamnolipid congener, Rha-Rha- C_{10}-C_{10} is considered to be the most common of its class (Abdel-Mawgoud *et al*., 2011) and a higher percentage of di-rhamnolipids is produced when hydrophilic substrates such as hydrocarbons are used during synthesis.

Surfactin, is predominantly secreted by *Bacillus subtilis* and its chemical structure consists of a cyclic lactone ring surrounded by seven amino acid residues interlinked with a β- hydroxyl fatty acid whose chain length varies from 12 to 16 carbon atoms (Figure 1C). Surfactin adopts a β turn, and forms

a β helical sheet and the amino acid sequence is expressed as LLDLLDL and surrounded by a heptapeptide ELLVDLL (Kakinuma *et al*., 1969). Additionally, the hydrophobic amino acid residues are situated at positions 2, 3, 4, 6 and 7 while negatively charged amino acid residues are situated at positions 1 and 5(Hue *et al*., 2001; Tang *et al*., 2010).

Gorin *et al*., (1961) identified the yeast fungi, *Candida apicola* as a producer of sophorolipids. Since then, sophorolipids have been found to be secreted extracellularly from several other non-pathogenic yeasts, however, *Candida bombicola* has been the subject of many investigations. Sophorolipids exist as acidic or lactonic forms, with the latter resulting from internal esterification of the carboxylic acid group to a lactone ring. Additionally, structural variations could exist as a result of differences in hydroxylation of the terminal carbon atom via acetylation of the hydroxyl sophorose sugar at C6', C6'' or C4'' which may be diacetylated, monoacetylated or deacetylated. Structural variation could also be due to the possession of one or more saturation bonds. Lactonic sophorolipids (Figure 1D) are non-ionic BSs, however, the acidic forms can be converted into anionic, cationic, or zwitterionic forms by coupling the carboxylic end with di-carbodiimide. Sophorolipid isoforms exhibit different biological and chemical behaviours. For example, lactonic sophorolipids have better surface tension with cytotoxic, biocidal, spermicidal and hydrophobic properties while acidic sophorolipids have better foaming, detergent, solubility, cosmetic and bio-remediation properties.

Due to their structural novelty and diverse biophysical properties, lipopeptides, glycolipids and other BSs have recently emerged as possible broad-spectrum agents for cancer chemotherapy (Gudiña *et al*., 2013). The cytotoxic activity of the selected BSs on cancer cells has been reported by a number of studies (Zhao *et al*., 2013; Thanomsub *et al*., 2006; Christova *et al*., 2010; Cao *et al*., 2011; Cao *et al*., 2009a; Cao *et al*., 2009b; Duarte *et al*., 2014; Rashad *et al*., 2014; Ribiero *et al*., 2015; Jing *et al*., 2006). However, the pharmacological effects of BSs on blood derived monocytic cancer cells has not been reported. In this study, the biological (e.g. anti-cancer) activities of these BSs is of particular interest. Furthermore, this research sheds new light on the action of lactonic sophorolipids on breast cancer cells. The aim of this work therefore was to functionally characterise the physico-chemical properties and systematically compare the surface active properties and cytotoxicity of the four selected biosurfactants against blood derived and breast cancer cell lines using MTT assay.

2. MATERIALS AND METHODS

2.1. Chemicals and reagents

R-95™ rhamnolipid (BS1a), R-90™ rhamnolipid (BS1b), surfactin (BS2) and 1′, 4″-sophorolactone 6′, 6″-diacetate (BS3) from yeast**,** doxorubicin hydrochloride, penicillin/streptomycin and MTT (3-[4,5-dimethyl-2-thiazolyl]-2,5-diphenyl-2H-tetrazolium bromide) were purchased from Sigma Aldrich (Gillingham, UK). Dulbecco's modified eagles medium (DMEM), supplemented with 10% heat inactivated foetal bovine serum [Origin: EU approved (South American)] in PET bottle were obtained from Gibco, UK. All other reagents were of analytical grade and used as received.

2.2. Physico-chemical characterisation

2.2.1. Attenuated total reflectance Fourier transform infrared spectroscopy (ATR-FTIR)

Before ATR-FTIR analysis the diamond crystal surface was cleaned and background spectra were collected. Samples were individually placed with just enough material to cover the crystal area. The pressure arm was positioned over the sample area and the arm of a Spectrum 100 series universal ATR accessory was locked into a precise position above the diamond crystal. This allowed force to be applied to the sample to ensure proper contact with the diamond crystal. IR spectra were collected between 400 and 4000 wave numbers (cm^{-1}) at a scan rate of 0.2 using a Perkin Elmer UATR Two infrared spectrometer.

2.2.2. High performance liquid chromatography (HPLC)

HPLC analysis was carried out for surfactin (BS2) and sophorolipid (BS3), both of which possess a UV chromophore, using an Agilent 1200 HPLC system composed of vacuum degasser, auto sampler, quaternary pump, UV-detector and an electronic integrator (HP Chemstation software rev A.09). An aliquot (20 µl) of the standard BS2 solution was injected onto a reversed-phase Gemini C18 column (250 x 4.6mm internal diameter; 5 µm particle size) (110A S/N 267789-48) held at room temperature. The mobile phase was flushed through the system for 10 minutes before beginning each run, and the samples were then eluted using an isocratic mobile phase composed of acetonitrile (0.1%) : trifluoroacetic acid (TFA) in deionised water (70:30, *v/v*) at a flow rate of 0.7 ml/min. The eluted components were detected using UV at a wavelength of 210 nm. The BS3 solutions were analysed using the same column and mobile phase as for BS2 but with mobile phase flow rate of 0.5 ml/min and detection wavelength at 205 nm.

2.2.3. Liquid chromatography mass spectrometry (LC-MS)

2.2.3.1 HPLC/ESI-MS of rhamnolipids

Compositional analysis of 95 (BS1a) and 90% (BS1b) rhamnolipids were performed by modifying (Déziel *et al*., 1999) HPLC/ESI-MS method. Briefly, 0.1 mg/ml of BS1a and BS1b were prepared in methanol and 1 µl was injected onto a Micromass Quattro Ultima (Waters, Wilmslow, UK) triple quadrupole mass spectrometer system using a 10 cm x 2.1 mm Supelco Ascentis Express (Supelco, Bellefonte, PA, USA) C18 reverse phase column (particle size 2.7 µm) in a mobile phase reverse phase gradient composition of A: water + 0.1% (v/v) formic acid and B: acetonitrile + 0.1% (v/v) formic acid. The gradient conditions were set as follows: initial composition of A : B (75 : 25), A : B (50 : 50) at 30 min, A : B (10 : 90) at 45 min, A : B (10 : 90) at 50 min, A : B (75 : 25) at 70 min and a re-equilibration of A : B (75 : 25) for 20 min. The mobile phase flow rate was 0.25 ml/min which was not split. Experiments were conducted using an electrospray ionization (ESI) source operated in negative ion

mode with a capillary voltage of 3.2 kV, cone voltage of 15 V, source and probe temperatures at 150°C and desolvation temperature of 400°C while the scanning mass range was from 50 - 900 *m/z* units.

2.2.3.2 HPLC/ESI-MS/MS of surfactin

Compositional analysis of BS2 was performed by modifying a previously reported HPLC/ESI-MS/MS method (Pecci *et al*., 2010). Briefly, 0.1 mg/ml of BS2 was prepared in a mobile phase (see below) and 1 µl was injected on to a Waters (Manchester, UK) ACQUITY UPLC® BEH C18 column (particle size: 1.7 µm). A mobile phase gradient was employed with composition of A: water + 0.1% (v/v) formic acid and B: acetonitrile + 0.1% (v/v) formic acid. The flow rate was 0.5 ml/min to the electrospray source. The gradient conditions were an initial composition of A : B (50 : 50) , A : B (50 : 50) at 0.34 min, A : B (0 : 100) at 2.38 min, A : B (0 : 100) at 2.95 min, A : B (50 : 50) at 3.00 min and a re-equilibration of A : B (50 : 50) at 5 min. No splitter was used, so the entire flow was introduced to the electrospray source and the UPLC column temperature was maintained at 40ºC throughout the run. Experiments were conducted using an electrospray ionization (ESI) source operated in positive ion mode with a capillary voltage of 1.5 kV. Initially, 15 V cone voltage was used to generate typical MS data confirming elution order, approximate purity profile and mass analysis. Consequently an elevated cone voltage of 100 V was used to generate pseudo MS/MS spectra on a Waters QDA single quadrupole mass spectrometer. The source and probe temperatures were at 120°C and 600°C respectively while the scanning mass range was from 100 - 1250 *m/z* units.

HPLC/ESI-MS of sophorolipids

Compositional analysis of BS3 was performed by modifying a previously HPLC/ESI-MS and HPLC/ESI-MS/MS method (Ribeiro *et al*., 2015). Briefly, 5 mg/ml of BS3 was prepared in a mobile phase (see below) and 1 µl was injected on to a Waters (Manchester, UK) ACQUITY reverse phase chromatography system using an ACQUITY UPLC® BEH C18 column (particle size: 1.7 µm) in a mobile phase gradient composition of A: water + 0.1% (v/v) formic acid and B: acetonitrile + 0.1% (v/v) formic acid. The flow rate was 0.25 ml/min to the electrospray source and the gradient conditions were an initial composition of A : B (50 : 50), A : B (50 : 50) at 0.6 min, then A : B (40 : 60) at 3.2 min, A : B (0 : 100) at 5.7 min, A : B (0 : 100) at 6.9 min, A : B (50 : 50) at 8.2 min and a re-equilibration of A : B (50 : 50) at 10 min. No splitter was used, so the entire flow was introduced to the electrospray source and the UPLC column temperature was maintained at 40ºC throughout the run. Experiments were conducted using an electrospray ionization (ESI) source operated in positive and negative ion mode with a capillary voltage of 1.5 kV and cone voltage of 15 V on a Waters QDA UPLC single quadrupole. The source and probe temperatures were set at 120°C and 600°C respectively while the scanning mass range was from 100 - 800 *m/z* units.

For all LC-MS analyses, nitrogen was used as both nebulizer and cone gas and supplied at a pressure of approximately 6 bars.

2.3. Measurement of critical micelle concentration (CMC) and minimum surface tension

The surface tension and critical micelle concentration (CMC) of BS1a, BS1b, BS2 and BS3 were measured. These biosurfactants have chain lengths of 12-18 carbon atoms, a range over which only BS1a and BS1b are soluble at room temperature, while BS2 and BS3 were soluble in Tris HCl buffer at pH 8.5. The surface tension measurements were undertaken at a temperature of 25 ± 1°C using a bubble pressure tensiometer (SITA Science on-line t60, Germany), calibrated by reference to de-ionised water (Mansour *et al*., 2015). Surface tension was recorded at a bubble life time value of 10,000 sec. Their surface tensions decrease with increasing concentrations until their CMC's are reached above which their plateau surface tensions are as low as 26.9 mN/m indicating excellent surface activities.

2.4. Cell-growth curves

2.4.1 Trypan blue growth curve for MCF-7 and HEK 293

Once the cell lines reached 80 to 90% of confluence, cells were seeded in 96 well plates (100 µl/well) at concentrations of $5x10^4$ cells/ml, $1x10^5$ cells/ml and 2.5 x 10^5 cells/ml for HEK 293, MCF-7 and THP-1 respectively. Plates were incubated at 37° in a CO_2 incubator over a period of 10 days. Samples from each cell line were collected after 4 hr and daily thereafter. Adherent cells were first detached via trypsin, then stained with trypan blue (TB) at a 1:2 dilution and counted in a Neubauer hemocytometer. Non adherent cells were directly stained with TB at a 1:2 dilution and counted in a Neubauer hemocytometer. Each experiment was carried out in triplicates(n = 3).

2.4.2. MTT growth curve for MCF-7 and HEK 293 cells

Cells were plated as above and after 4 hr incubation and daily thereafter, 10 µl of 3-[4, 5-dimethyl-2-thiazolyl]-2, 5-diphenyl-2H- tetrazolium bromide (MTT) reagent was added to three wells and incubated for a further 4 hr. Subsequently, 75 µl of supernatant media was discarded from each of the wells after which 50 µl of DMSO was added to solubilize the formazan formed in the treated wells. The plate was incubated for 10 min and analysed on a plate reader at 540 nm. Each experiment was repeated three times (n = 3).

2.5. Cytotoxicity studies

2.5.1 Cytotoxicity against HEK 293 and MCF-7 and cells

Cytotoxicity of BS1a, BS1b, BS2 and BS3 and doxorubicin hydrochloride (DOX) (Sigma Aldrich, UK) against non-cancerous human embryo kidney (HEK293, ECACC 85120602), human Caucasian breast adenocarcinoma (MCF-7 ECACC number 86012803) cell lines obtained from American Tissue and Cell Culture (ATCC), were determined by MTT (Sigma Aldrich, UK) assay according to the optimised protocol below. HEK293 and MCF-7 were sub-cultured in Dulbecco's modified eagles medium (DMEM), and all were supplemented with 10% heat inactivated foetal bovine serum (Gibco, UK) and

1% penicillin/streptomycin (Sigma Aldrich, UK). HEK 293 and MCF-7 cells suspended in 100 µl DMEM medium were seeded in 96 well plates at a concentration of 10^5 cells/ml and incubated at 37°C in 5% CO_2 for 24 hr. Both cells were then treated with the BSs and DOX at different concentrations using DMEM as diluting solution. After 24, 48 and 72 hr respectively, 10 µl of 5 mg/ml MTT in PBS solution was added to the wells and the cells were incubated for another 4 hr at 37°C. The positive and negative controls (untreated cells and cell treated with BSs and DOX) were included in the assay. The formation of formazan was measured using a multiscan EX microplate photometer at 540 nm. Cell viability was calculated according to the following equation:

$$\text{Cell viability (\%)} = (A_{Tr}/ A_{UTr}) \qquad \text{Equation 1}$$

where A_{Tr} is the absorbance of cells treated with BSs and DOX and A_{UTr} is the absorbance of untreated cells. IC_{50} value was calculated from dose-response curves of the cell viability versus concentration graphs, plotted using GraphPad Prism 5.

2.5.2. Cytotoxicity against THP-1 cells

Cytotoxicity of BS1a, BS1b, BS2 and BS3 and DOX against human leukemic monocyte (THP1, ECACC number 88081201) cell lines obtained from American Tissue and Cell Culture (ATCC), was also determined by MTT assay according to the optimised protocol below. THP-1 cells were grown in RPMI 1640 medium (Sigma Aldrich, UK) supplemented with 10% foetal bovine serum (heat inactivated) (Gibco, UK) and 1% penicillin/streptomycin (Sigma Aldrich, UK). The THP-1 cells suspended in 50 µl RPMI 1640 medium were seeded in 96 well plates at a concentration of 5 x 10^5 cells/ml and incubated at 37°C in 5% CO_2 for 24 hr. Cells were then treated with 50 µl each of the four BSs and DOX at different concentrations using RPMI 1640 as diluting agent. After 24, 48 and 72 hr, respectively, 10 µl of 5 mg/ml MTT in PBS were added to the wells, and the cells were incubated for another 4 hr at 37 °C. After the 4 hr of incubation with MTT reagent, the THP-1 cells were spun down at 600 g for 5 min. Finally, 100 µl of DMSO was added after 75 µl of media supernatant had been withdrawn.

The formation of formazan was measured using multiscan EX microplate photometer at 540 nm as described above and cell viability calculated using equation 1 above.

2.5.3. Data analysis and calculation of IC_{50} values

All numerical biological data was analysed using GraphPad Prism 4. IC_{50} values were extrapolated from dose–response curves using the sigmoidal–dose response (variable) model. To obtain the IC_{50} values, dose-response curves of the % viability were generated using a four-parameter nonlinear regression with either variable or fixed slope (Prism, GraphPad). Using a constrained or fixed Hill slope of -1, bottom and top plateaus of 0 and 100 respectively, BSs and DOX concentrations were log transformed

and the % viability was plotted using nonlinear regression. This analysis with a fixed Hill slope provided the parameter of potency (IC_{50}) but without the index of cooperativity as the Hill slope was standardized.

3. RESULTS AND DISCUSSION

3.1. Physico-chemical characterization

The physico-chemical properties of the four BSs were characterised using various analytical techniques to confirm their structural characteristics, which are essential for confirming their identity and functional activity.

3.1.1 ATR-FTIR spectroscopy

3.1.1.1 ATR-FTIR spectra of 95% and 90% rhamnolipids

The dominant absorbance bands of the two rhamnolipids (BS1a and BS1b) are shown in (Figure 2) below. The strong, broad bands around 3331-3335 cm^{-1} are attributed to hydrogen bonding and O-H stretching of the hydroxyl groups. The double bands centred at 2925-2928 cm^{-1} are assigned to asymmetric stretches for CH (in CH_2 groups) whilst those centred at 2855-2856 cm^{-1} are derived from symmetric C-H stretching vibrations of aliphatic groups such as those represented in the hydroxydecanoic acid chain tails. A C=O stretching band at 1731 cm^{-1} is characteristic of ester bonds and carboxylic acid groups. In the fingerprint region of the spectrum, the area between 1445-1380 cm^{-1} represents C-H and O-H deformation vibration, typical for carbohydrates as in the rhamnose units of the molecule. The lower range of the fingerprint region below 1200 cm^{-1} represents different kinds of C-H, C-O and CH_3 vibrations which cannot be allocated more specifically (Zhao *et al*., 2013). It should be noted that the above reference used rhamnolipids obtained from different model organisms, culture and purification conditions and this accounts for the slight differences in the IR spectra of samples used in this study and those reported in Zhao *et al*., 2013.

3.1.1.2 ATR-FTIR spectrum of surfactin

The IR spectra of surfactin (BS2) (Figure 2) were evaluated with focus on the main bands. The absorption band centred at 3300 cm^{-1} corresponding to the N-H stretch can be attributed to peptide residues. Another intense band with maxima of 2957 cm^{-1} and 2927 cm^{-1}, corresponding to the C–H (CH_3) and (CH_2) stretch, can be associated with the lipopeptide portion of the molecule. At 1719 cm^{-1}, a medium intensity band is observed that can be related to the absorption of C=O groups from lactonization. At 1643 cm^{-1}, a CO–N stretch band is attributed to the amide group while bands at 1467 cm^{-1} and 1387 cm^{-1} indicate aliphatic chains (-CH_3-CH_2). These results agree with the analysis of Sousa and co-workers (2014) and suggest that the surfactin employed in this study was of the expected standard.

3.1.1.3 ATR-FTIR spectrum of sophorolipids

The dominant absorbance bands for sophorolipids (BS3) are shown in (Figure 2). The spectra revealed broad bands at 3406 cm^{-1} which correspond to O-H stretching, while asymmetrical and symmetrical stretching of methylene occurred at 2927 cm^{-1} and 2856 cm^{-1} respectively. The absorption band at 1744 cm^{-1} was attributed to C=O stretching from lactone esters or acids. The bands at 1451cm^{-1} corresponded to the C-O-H in the plane binding of carboxylic acids (-COOH). The C=O absorption band from acetyl esters was observed at 1232 cm^{-1}, while the stretch of C-O band for C (-O)-O-C in lactone groups can be observed at 1166 cm^{-1}. The C-O stretch from C-O-H groups of sugar (sophorose moiety) was observed at 1071 cm^{-1}. Finally the IR spectra revealed the absorption band for C=C at 721 cm^{-1}. With the exception of the band at 3406 cm^{-1} which corresponded to the O-H stretch, all structural details analysed were found to be similar to those reported by (Rashad *et al*., 2014).

Comparison of IR spectra between the different BSs

As a result of different chemical structures (Figure 1), the BSs showed different FTIR fingerprints. BS2 showed very distinct pattern between 400-1600 cm^{-1} which may be due to the lack of sugar residues and the presence of amide (-CO–N stretch) at 1643 cm^{-1} and an unassigned shoulder at 1467-1387 cm^{-1}. BS1a and BS1b (representing both rhamnolipids) had bending of O-H bands in the carboxylic acid group at 1445-1370 cm^{-1}, (C-O-C stretching of rhamnose sugars with a shoulder and pyranyl 1 sorption band 1232-1034 cm^{-1} (shoulder) (C-O-C stretching in the rhamnose), (pyranyl 1 sorption band) and (α-pyranyl II sorption band at 916 cm^{-1} and 806-838 cm^{-1} respectively. On the other hand, BS3 had [(C-O-H in plane binding of carboxylic acids at 1451 cm^{-1}, C=O absorption band due to acetyl esters at 1232 cm^{-1}, (C-O band of C (-O)-O-C due to lactones) at 1166 cm^{-1}, (C-O stretch from C-O-H sophorose sugars at 1071 and 721 cm^{-1} (C=C)]. Details of the differences in the FTIR profiles of the four selected biosurfactants, are summarised in Tables A1 and A2 in the supplementary data in the appendix section.

3.1.2. High performance liquid chromatography (HPLC)

As the selected BSs will be incorporated into novel drug delivery systems to test their release for biological activity, HPLC was used to analyse surfactin and sophorolipids since they possessed chromophores which allowed UV detection during.

3.1.2.1 Surfactin

As will be expected of a microbial derived biosurfactants, the standard surfactin showed a complex mix of different isoforms and Figure 3A shows that the sample contained nine isoforms, which eluted between 26 and 67 min. Of these isoforms, seven were major, namely, peaks 1, 2, 3, 4, 5, 7, 8, and two were minor, namely, peaks 6 and 9. In addition, Figure 3A shows that the peaks were well separated except isoform peaks 2 and 3, which differed in their retention times by less than 1 min (at 33.16 and

34.10 min respectively). Once the conditions had been optimised, HPLC was repeated 10 times for the purpose of reproducibility and the standard deviation between the 10 runs was 0.94. This result was in accordance with that obtained by (Abdel-Mawgoud *et al*., 2008), and therefore deemed acceptable.

3.1.2.2 Sophorolipids

Standard sophorolipid (Figure 3B) contained two major isoform peaks, which eluted between 13 and 17 min. The figure shows that the peaks were well separated and differed in their retention times by about 4 min. Once the conditions had been optimised, HPLC was repeated 10 times for the purpose of reproducibility with a standard deviation of 0.03 which was deemed acceptable.

3.1.3. Liquid chromatography mass spectrometer (LC-MS)

LC-MS was used to characterise the selected biosurfactants, which was particularly useful for the two rhamnolipids (BS1a and BS1b) due to their lack of a functional chromophore.

3.1.3.1 95% and 90% rhamnolipids

Seven main peaks were obtained from the LC-MS spectra of BS1a (Figure 4A & 4C) at *m/z* values of 175.1, 233.4, 621.8, 649.9, 503.6, 677, and 175.1 respectively. However, the peaks at *m/z* 175.0 which occurred at retention times of 0.74 and 63 min could not be assigned and did not correspond to any congeners found in literature and therefore suspected to be noise. The most abundant ions were found at *m/z* 649.9 and 503.6 which have been identified as the (Rha_2-C_{10}-C_{10}), and (Rha-C_{10}-C_{10}) congeners, respectively (Déziel *et al*., 1999; 2000). On the other hand, nine main peaks were obtained from the LC-MS spectra of BS1b (Figure 4B & 4D) at *m/z* values 181.1, 621.7, 475.7, 650.0, 649.9, 503.7, 677.8, 531.7, 191.1 respectively. However, as was the case for BS1a, the peaks at *m/z* 181 and 191 which occurred at 0.74 and 63 min were not assigned and did not correspond to any congeners found in literature. Further, the most abundant ion was an unassigned peak at *m/z* 650.0 with a relative abundance of 23%. This was followed by *m/z* 677.0 which was identified as the isomeric pair Rha_2-C_{12}-C_{10}/ Rha_2-C_{10}-C_{12} with a relative abundance of 19.3%. The peaks at *m/z* 503.7 and 649.9 were identified as (Rha-C_{10}-C_{10}) and Rha_2-C_{10}-C_{10} with elution times of 40 and 37 min, respectively. However, unequivocal identification would only be possible if tandem–MS/mode is employed.

The most predominant components for 95% and 90% rhamnolipids correlated with the results from Zhao *et al*., 2013, which were obtained from crude extracts analysed by ESI-MS. In their study, the mass spectrum of mono-rhamnolipid (R_1) showed intense molecular ions at *m/z* 333, 475, 503 and 529 with molecular ion at *m/z* 503 as the predominant component, which corresponded with the known structure of mono-rhamnolipids. On the other hand, their mass spectrum of di-rhamnolipid (R_2) samples showed the presence of signals at *m/z* 479, 621, 649, 677 and 685 with predominant ion at *m/z* 649 corresponding to di-rhamnolipids. Tandem-MS/mode was used to unequivocally identify the predominant R_1 ion as Rha-C_{10}-C_{10} which showed daughter ions at *m/z* 333 corresponding to a ruptured

ester link, *m/z* 169 corresponding to breaking of fatty acid chain and *m/z* 163 corresponding to the fragmented link in the rhamnose-alkyl chain. In the case of R_2, the major molecular ion with *m/z* 649 was identified as Rha_2-C_{10}-C_{10} which gave daughter ions at *m/z* 479 corresponding to a rupturing of the ester link to give Rha-C_{10} and hydroxyl decanoate (*m/z* 169) as well as another daughter ion at *m/z* 163 corresponding to a single rhamnose. The congeners in this research were further confirmed on the basis of (Deziel *et al*., 1999) who reported the synthesis of rhamnolipids from two separate cultures grown on mannitol and naphthalene. For the mannitol culture, twenty eight congeners were identified although most were in trace amounts. However, the pseudo molecular ion at *m/z* 475 was the base peak but some fragment ions were observed at *m/z* 305, 311 and 333. Further, collision induced fragmentation in their study revealed that the pseudo molecular ion at *m/z* 475 were the isomers Rha-C_8-C_{10} and Rha-C_{10}-C_8 which co-eluted under negative electrospray ionization. Additionally, *m/z* 305 and 333 ions were cleaved at the 3-carbon-oxygen bond to give corresponding daughter ions at *m/z* 141 and 169 respectively. Furthermore, *m/z* 163 produced by the cleavage of the rhamnose moiety was common to both BS1a and BS1b. The predominant ion was identified as Rha-Rha-C_{10}-C_{10} with a relative abundance of 56.9%. While the most abundant 3-hydroxy fatty acids were C_8, C_{10}, and C_{12}, unsaturated $C_{12:1}$ and $C_{14:1}$ rhamnolipids were also observed.

In a further study (Deziel *et al*., 2000) comparing LC-MS with direct infusion which did not require prior chromatographic separation, 23 congeners were identified, with Rha-Rha-C_{10}-C_{10}, Rha-C_{10}-C_{10}, Rha-C_8-C_{10}, Rha_2-C_{10}-C_{12} and Rha-C_{10}-$C_{12:1}$ and Rha_2-C_{10}-C_8 being the most abundant. Christova *et al*., (2011) detected mono- and di-rhamnolipid congeners as anions at *m/z* values of 503 and 649, which corresponded to the deprotonated molecules of Rha-C_{10}-C_{10} (mono-rhamnolipid) and Rha_2-C_{10}-C_{10} (di-rhamnolipid) respectively. When both congeners were subjected to further tandem–MS mode, the pseudo molecular ion at *m/z* 503 produced two major fragment peaks at *m/z* 333 and 339 corresponding to ruptured ester links as well as *m/z* 169 corresponding to released fatty acid. However, the fragmentation of the main pseudo molecular ion at *m/z* 649 produced daughter ions at *m/z* 479 corresponding to the rupture of the ester bond between the two alkyl chains in dirhamnolipid. The other characteristic ions they detected were *m/z* 339 representing the cleavage of the link between the rhamnose and alkyl moiety as well as a daughter ion at *m/z* 163 corresponding to the single rhamnose detected.

3.1.3.2 Surfactin

The sample provided was nominally of 98% purity with a given molar mass of 1036.34 g/mol. Multiple peaks, were observed in the extracted ion chromatogram, suggesting that several structural isomers are present. These peaks were independently resolved into eight mass spectra. The structural isomers resolved from each mass spectra were putatively assigned to members of surfactin family based on literature as summarised in Table A3 of the appendix. The heterogeneity in the Leu/Ile at the 2nd and 7th position, respectively of the peptide sequence of surfactin is well established. However,

resolution of Leu and Ile using LC- MS is quite challenging. Therefore, surfactin was further characterised by tandem mass spectrometry at higher cone voltage of 100 V, however, the fragmentation pattern was observed to predominantly match the results obtained at lower voltage. The peaks at *m/z* 995, 1009, 1023, 1037, 1051 may represent the $[M + H]^+$ ions of the same surfactin basic structure but with difference in mass of 14 Da, suggesting that the metabolites produced during microbial synthesis differ only in the length of the fatty acid chain component.

Alkali metal ion (e.g. Na^+) adducts are a common feature in the mass spectra of surfactin, by binding of the metal ion to free carboxylic acid groups in the biosurfactant. The sodium and potassium adducts of surfactin are the most common, as these metal ions are ubiquitously present in nature (Hue *et al*., 2001; Vater *et al*., 2002). The addition of chloride salts of these metals to surfactin samples, greatly enhances the relative intensity of corresponding metal ion species in the mass spectra (Hue *et al*. 2001; Williams and Brodbelt, 2004). The precursor ions *m/z* 1017, 1031, 1045, 1059 and 1073 can be attributed to sodium ion adducts of surfactin homologues with *m/z* 995, 1009, 1023, 1037 and 1051, (Figures A1 and A2). The precursor ion *m/z* 1061 in the mass spectra (data not shown) can be attributed to potassium adduct of surfactin homologue with *m/z* of 1023. The absence of any strong basic amino acids in surfactins preferentially make peptide bonds and ester groups to be protonated, and thus making them susceptible targets for intra-molecular nucleophilic cleavage reactions mediated by –C=0 groups adjacent to these protonated sites.

3.1.3.3 Sophorolipids

The sophorolipid sample provided was nominally of 70% purity with a given molar mass of 688 g/mol thus providing a protonated ion of *m/z* of 689. Figure A3 in the appendix (supplementary data) shows the total ion chromatograms and Figure 5 shows a representative mass spectrum of the sophorolipid sample analysed. Multiple peaks, 1 – 7, containing *m/z* 689 can be observed in the extracted ion chromatogram, along with the sodiated adduct at *m/z* 711, suggesting that several structural isomers were present. In the 0-100% ion chromatogram, seven peaks were eluted, although three of them co-eluted together with overlapping signals. Only three of the peaks (1^{st}, 3^{rd} and 7^{th}) observable in the 0-100% ion chromatogram are among the mass spectrum of the isomers. The second chromatographic peak at retention time of 2.34 min had a shoulder on the left side of the peak resulting from a co-eluted peak at 2.26 min. These peaks were independently resolved into seven mass spectra all of which showed other masses not observed in the ion chromatogram, however, individual identification of each *m/z* peak was beyond the scope of the current study.

3.1.4. Critical micelle concentration and surface tension

The critical micelle concentration (CMC) is the point at which the amount of surfactant added to solutions begins to form micelles whilst surface tension (ST) is a measure of the work required to bring a molecule from the bulk phase to the surface (Rosen, 1978). Table 1 shows comparative CMC and

minimum ST data of the four BSs analysed. The CMC values of the BSs were significantly lower in comparison with chemical surfactants such as sodium carpylate which has a CMC value of 1805 mg/L (Stanley *et al*., 2009). The surface tension of water is 72.75 mN/m (at 20°C) and good BSs can reduce surface tension of water to 35 mN/m, (Manivasgan *et al*., 2014). This is interesting and suggests that the BSs used in this study possessed excellent surface lowering properties with surface tension ranging between 26.00 – 32.96 mN/m. Rhamnolipids have been found to reduce the surface tension of water to 26.90 mN/m at a CMC of 51.50 mg/L (Nitschke *et al*., 2005), surfactin to 27.00 nN/M at a CMC of 10 mg/L (Yeh *et al*., 2005) and sophorolipids to 33.50 mN/m at CMC of 9.50 mg/L (Joshi-Navare, 2013) and all these reported values correspond to the data obtained in this research as shown in (Table 1). The CMC of ionic detergents is determined by the combined effect of the repulsive and hydrophobic interaction effect on membrane proteins and lipids by their head and tail groups respectively. A detergent is a small amphiphilic molecule which when added to the solution surrounding a lipid bilayer, interacts with the hydrophobic tails of the lipids. If the interacting membrane contains proteins, (e.g. cell membrane), the hydrophobic tails of the detergent molecules also interact with the hydrophobic parts of the membrane proteins. As a result of this the detergent tends to disrupt the bilayer.

Table 1 CMC and corresponding minimum ST (n = 3, ± SD) values of the four selected BSs.

Surfactants	CMC (µg/ml)	Minimum S.T. (mN/m)
BS1a	4.78	27.20 (0.06)
BS1b	6.01	26.00 (0.17)
BS2	16.90	26.90 (0.10)
BS3	7.68	32.96 (0.05)

Consequently, the detergent molecules confer biocidal properties by displacing cell membrane phospholipids and end up forming water-soluble detergent-protein complexes. Ortiz *et al*., (2006), described the molecular interaction between the phospholipid acyl chains of a phosphatidyl choline membrane and produced di-rhamnolipid molecule as a consequence of the intercalation between the di-rhamnolipids and phospholipids. The alignment of the hydrocarbon chains of the di-rhamnolipid with the phospholipids acyl chains can disrupt the phospholipid packing, reduce cooperativity of the transition and shift the phase transition temperature to lower values. Rhamnose is a deoxy sugar, sophorose is a disaccharide while leucine, asparagine and glutamic acid are amino acids present in surfactin, as opposed to the amino sugar in doxorubicin. It is hypothesised that their amphiphilic parts fuse with the phospholipid bilayer of the cell membrane via passive diffusion to exert a detergent-like effect that disrupts the plasma membrane. The double bonds and length of hydrocarbon chain contained in microbial biosurfactants may reduce the strength of hydrophobic interactions and disrupt the phospholipid packing of the membrane bilayer. In this research, the four biosurfactants had hydrocarbon tails in the order of BS3 > BS2 > BS1b/ BS1a (elucidated by MS data). The sophorolipids tested in this

study has a chain length of 18 carbon atoms followed by surfactin which varied in chain length from 12-16 carbon atoms and rhamnolipids with 2 double chains of 12 carbons atoms. It is hypothesised that these hydrocarbon chains forms mixed micelles with the phospholipid bilayer to exert a detergent-like effect that disrupts the plasma membrane. This is consistent with the CMC of BSs recorded in (Table 1). Generally, the CMC should decrease with increasing surfactant chain length, however, this was not the case in the current study. The reason might be because the biosurfactants studied in this research are not single component entities and possibly possessed minor components (congeners) of different chain lengths in addition to the expected chain length congeners. For example BS1a is a mixture of both di-rhamnolipids and mono-rhamnolipids. Further, the LC-MS data for some of the biosurfactants (e.g. BS1b) showed very prominent congeners which could not be assigned and all these which may affect its CMC values. However, this requires further investigation to confirm this possibility or otherwise.

3.2 Cytotoxicity of biosurfactants

3.2.1. Growth curves

The aim of this section was to determine the growth curves for three cell lines to identify optimal log phase for testing with the BSs. It was important to analyse the behaviours of the individual cell-lines, to inform the subsequent evaluation of the anti-proliferative effects of the selected BSs. The growth curves for MCF7 and HEK 293 cells were determined using TB and MTT assays, while the non-adherent cancerous THP-1 cell was observed using TB assay only. Further discussion can be found in the supplementary data section (A1) of the appendix.

3.2.2 Dose response curve of biosurfactants on HEK 293, MCF-7 and THP-1

MTT assay was carried out on three cell lines following 24, 48 and 72 hr of exposure to the BSs and showed significant changes in cell proliferation at the different time points as outlined below. The chemotherapy agent DOX employed as positive control showed IC_{50} values depicting more potency than all the BSs which is to be expected. The cytotoxicity profiles of BS1a, BS1b, BS2, BS3 and DOX against THP-1 are shown in Figure 6 whilst the profiles of the most potent BS (BS3) against MCF-7 are shown in Figure 7. The corresponding IC_{50} values of all the BSs and DOX against the three cell lines are summarised in Table 2 below. More detailed discussion for activity of the BSs and DOX against the two cancerous cell lines (THP-1 and MCF-7) is provided below.

Table 2 IC_{50} of BSs and DOX on HEK 293, MCF-7 and THP-1

Drugs	THP-1			MCF-7			HEK 293		
	24	48	72	24	48	72	24	48	72
BS1a	176.20 (0.12)	59.52 (6.12)	48.71 (0.12)	153.40 (0.12)	98.27 (0.13)	33.08 (0.90)	61.65 (7.47)	209.40 (0.10)	83.91 (4.07)
BS1b	61.97 (0.10)	14.47 (0.24)	8.10 (0.36)	168.50 (0.17)	42.85 (0.16)	30.05 (0.16)	30.98 (4.31)	63.51 (0.13)	57.03 (0.15)
BS2	24.42 (0.23)	17.76 (0.24)	11.29 (0.28)	111.70 (0.12)	119.40 (0.17)	21.17 (0.20)	29.53 (0.18)	76.61 (14.48)	46.52 (0.14)
BS3	10.52 (0.18)	5.58 (0.26)	6.78 (0.24)	51.46 (0.16)	33.49 (0.15)	10.75 (0.23)	21.53 (0.20)	40.57 (8.11)	27.53 (1.03)
DOX	15.68 (1.16)	6.49 (0.63)	2.95 (0.36)	11.12 (0.77)	8.35 (0.64)	4.60 (0.49)	16.70 (0.66)	6.08 (0.54)	1.04 (0.43)

The table above shows comparative IC_{50} data of BSs and DOX on HEK 293, MCF-7 and THP-1 cells at different time points. Values were derived from fitting the data (n = 3) from graphs of percentage cell viability against drug concentration (µg/ml) from MTT assay. By constraining the slope of the curve, the error associated with the curve was reduced as demonstrated by narrow 95% confidence intervals for IC_{50} (data not shown). This conformed best to the requirements of logistic curve modelling resulting in no data exclusion.

3.2.2.1 Rhamnolipids (BS1a and BS1b)

Dose-response curves showed that BS1a had an IC_{50} of 33.08 µg/ml on MCF-7 cells after 72 hr (Table 2). This was a much lower cytotoxic effect compared to that obtained by (Zhao *et al*., 2013; Thanomsub *et al*., 2006), who reported values at 1 µg/ml and 6.25 µg/ml respectively after 48 hr. This may be due to the fact that BS1a is a mixture of both di-rhamnolipids and mono-rhamnolipids. Zhao *et al*., (2013) reported no activity when mono-rhamnolipids congeners and the crude extract were tested on MCF-7. However BS1b showed greater sensitivity on MCF-7 cells which may be due to the activity of the predominant congener which was unassigned from the LC-MS data. Cytotoxicity may also be due to the presence of the second most abundant congener which was the isomeric pair Rha_2-C_{12}-C_{10}/ Rha_2-C_{10}-C_{12}. This contradicts (Thanomsub *et al*., 2006) report that no activity was detected and therefore requires further investigation.

THP-1 showed sensitivity to BS1a at a concentration of 48.71 µg/ml after 72 hr, (Table 2) but a much greater effect was observed with BS1b after 48 and 72 hr with IC_{50} of 14.47 and 8.10 µg/ml respectively. These results differ from a previous study (Christova *et al*., 2012) on human pre-B leukemic line BV-173, T-cell chronic lymphocytic leukaemia SKW-3 and human promyelocytic leukaemia HL-60 cell lines. The IC_{50} they obtained for mono- (Rha C_{10}-C_{10}) and di- (Rha_2 C_{10}-C_{10}) rhamnolipid congeners after 72 hr exposure were (50, 54, 67) µM and (82, 108, 77) µM respectively indicating greater potency of mono-rhamnolipids in comparison to di-rhamnolipids. This may be due to the differences in composition of the different congeners, or cell line differentiations. BS1b appeared to be toxic to normal cells (Table 2) after 24 hr but this cytotoxicity decreased after 48 and 72 hr. The anticancer action of rhamnolipids (BS1a & BS1b) may be due to the capacity of their amphiphilic parts to fuse with the phospholipid bilayer to exert a detergent-like effect that disrupts the cell/ plasma membrane.

3.2.2.2 Surfactin (BS2)

Dose-response curves showed that BS2 had an IC_{50} of 21.17 µg/ml on MCF-7 cells after 72 hr (Table 2). This was a much lower cytotoxic effect compared to that obtained by (Cao *et al.*, 2011; Lee *et al*., 2012) who reported cytotoxicity at 30 µg/ml and 10 µg/ml respectively after 48 hr. This may be due to differences in potency because of different sources with the surfactin used by Cao *et al*., 2011; obtained from *Bacillus natto*, whilst that used (BS2) in the current study was an industry standard. THP-1 showed greater sensitivity to BS2 with IC_{50} of 24.42, 17.76 and 11.29 µg/ml after 24, 48 and 72 hr respectively, (Table 2) in comparison to that reported (Cao *et al*., 2009a) with a value of 19.1 µg/ml after 48 hr on human chronic myelogenous leukaemia (K562) cells. This may be due to culture conditions, or cell line differentiations. Further, BS2 appeared to be toxic to normal cells (Table 2) after 24 and 72 hr but this cytotoxicity decreased after 48 hr which may indicate a lag phase of the cells disrupted by external stimuli. Surfactins are characterised by the presence of four amino acids; leucine, valine, glutamic acid and aspartic acid in repeating d and l conformations to form a seven membered peptide ring attached to

a lactone fatty acid chain. According to (McClements, 2006), the force of electrical charges decreases with increasing ionic strength. Ionic interactions refer to the electrostatic forces between synergistic and repulsively charged groups. The exposure of numerous side chains may lead to cellular lysis by increasing the permeability of the membrane and metabolite flow. This is due to changes in the physical structure of the membrane through the alteration of its protein conformation which alters functions such as transport and generation of energy.

3.2.2.3 Sophorolipids (BS3)

Dose-response curves showed that BS3 had an IC_{50} of 33.49 and 10.75 (µg/ml) on MCF-7 cells after 48 and 72 hr (Table 2). However, (Rashad *et al*., 2014) reported no activity which may be due to the fact that the sophorolipids they tested were mixtures of acidic and lactonic congeners in comparison to the pure lactonic standard used in this research. Ribiero *et al*., (2015) on the other hand reported IC_{50} values of 30 µg/ml, 15 µg/ml, and 15 µg/ml of diacetylated sophorolipids on oncogene positive breast cancer cell line (MDA-MB-231), at 24, 48 and 72 hr respectively which was not much different from that observed against MCF-7 in the current study. However, THP-1 cells showed greater sensitivity to BS3 with IC_{50} of 10.5, 25.58 and 6.78 (µg/ml) after 24, 48 and 72 hr respectively, (Table 2). Further, BS3 was cytotoxic on HEK 293 cell lines with IC_{50} of 21.53, 40.57 and 27.53 µg/ml after 24, 48 and 72 hr respectively. Lactonic sophorolipids (BS3) contain a diacetylated disaccharide sophorose sugar moiety esterified to a long unsaturated fatty acid tail. The high potency of sophorolipid may be due to the lactonic form in contrast to previous reports using mixed isomers.

3.2.2.4 Doxorubicin (DOX)

Dose-response curves showed that DOX had an IC_{50} of 11.12, 8.35 and 4.60 µg/ml on MCF-7 cells after 24-72 hr. THP-1 showed greater sensitivity to DOX compared to the four BSs with IC_{50} values of 15.68, 6.48 and 2.95 µg/ml after 24, 48 and 72 hr respectively. Structure-activity relationships have shown an important role for the structure and stereochemistry of the aminosugar (daunosamine) on the pharmacological activity of anthracyclines related to DOX based on the evidence that blocking the amino function resulted in a substantial loss of cytotoxic activity and reduced DNA-binding affinity, (Arcamone *et al*., 1981; Zunino *et al*., 2001).

3.2.2.5 Selectivity index

Another important parameter to determine in cytotoxicity studies against cancer cell lines is the selectivity index (SI) which is the toxicity against cancerous cells of the compound of interest relative to normal cells (Assanga *et al*., 2013), in this case BSs and DOX against THP-1 relative to HEK 293 and against MCF-7 relative to HEK 293. With the exception of BS1b at 72 hr, all BSs showed highest selectivity for THP-1 at 48 hr in the order of BS3 > BS1b > BS2 > BS1a > DOX. Furthermore, after 24 and 48 hr, BS3 was the best as it had low IC_{50} (10.52, 5.58 µg/ml) and a high SI value (1.21, 7.27).

However, although BS3 had the best IC_{50} (6.78 µg/ml) followed closely by BS1b (8.10 µg/ml), after 72 hr, the SI of the latter was better than BS3 with values of 7.04 and 4.06 respectively. After 72 hr, the best SI observed on MCF-7 line followed the order of BS1a > BS3 > BS2 > BS1b > DOX. Interestingly, although BS3 had lower IC_{50} (10.75 µg/ml) after 72 hr, its SI of 2.38 was lower than that of BS1a (2.54) even though the latter had an IC_{50} of 33.08 µg/ml. In addition, although the positive control DOX, showed the highest anti-proliferative activity (with the exception of BS3), SI of DOX in the two cancerous cell lines was less than that of all the BSs evaluated, which indicates that they are more specific and effective for slowing the growth of the tested cancer cell lines and hence may be potential candidates for use in human cancer therapy. However, further investigations will be required in this regard to validate this hypothesis.

Table 3 SI of BSs and DOX on THP-1 and MCF-7 cell lines relative to that of the normal cells HEK 293 at different time points.

Compounds	**THP-1**			**MCF-7**		
	24 hr	48 hr	72 hr	24 hr	48 hr	72 hr
BS1a	0.32	3.52	1.72	0.40	2.13	2.54
BS1b	0.50	4.40	7.04	0.18	1.48	1.90
BS2	1.21	4.31	4.12	0.26	0.64	2.20
BS3	2.05	7.27	4.06	0.42	1.21	2.38
DOX	1.07	0.94	0.18	1.50	0.73	0.12

The table above compares selectivity index (SI) of BSs and DOX on THP-1/HEK 293 and MCF-7/HEK 293 cells at different time points. Order of THP-1 SI was BS3 > BS1b > BS2 > BS1a > DOX at (48 hr) with the exception of BS1b at 72 hr. Order of MCF-7 SI was BS1a > BS3 > BS2 > BS1b > DOX at (72 hr). No standard deviation is provided here since these were obtained by dividing average IC_{50} values from table 2 above.

4. CONCLUSIONS

This research investigated the functional physico-chemical properties and biological activity of four microbial derived BSs, 95% rhamnolipids (BS1a), 90% rhamnolipids (BS1b), surfactin (BS2) and lactonic sophorolipid (BS3). The hypothesis for their biocidal activity was that the BSs form mixed micelles which exert a detergent-like effect that disrupts the plasma membrane. There are few studies that systematically compare the anti-proliferative activity for structurally different BSs, determining doubling time (DT) and highest growth rate. The susceptibility to growth inhibition with BSs was greater in THP-1 than in MCF-7, likely because the THP-1 line has lower DT values and is a cell line with accelerated metabolism. The BSs tested in this study were toxic to normal cells at lower concentrations than cancerous cells, however, lactonic sophorolipid (BS3) showed the closest cytotoxicity to DOX and therefore has high potential application as an anticancer agent. The physico-

chemical characteristics of the selected BSs suggests that their mechanism of action may be due to biocidal activity on the cell membrane. The structural differences of the BSs and biological activities will be beneficial for the formulation of synergistic drug delivery. Future work will therefore explore the use of noisome based delivery systems incorporating the individual BSs and in combination to target them to the cell lines tested above to improve their specificity and therefore reduce their toxicity against non-cancerous cells. Further work will also involve testing the BSs loaded niosomes in other biological applications such as anti-inflammatory action for improving wound healing.

ACKNOWLEDGMENTS

The authors are grateful to Mrs Devyani Amin for her help with HPLC analysis, Dr Cris Lapthorn and Dr Iain Goodall for their help with LC-MS analysis and Omar Mansour for his help with the surface tension measurements.

FUNDING SOURCE

This research did not receive any specific grant from funding agencies in the public, commercial, or not-for-profit sectors.

5 REFERENCES

Abdel-Mawgoud, A.M. Hausmann, R., Le´pine, F, M€uller, M.M., De´ziel, E. 2011. Rhamnolipids: Detection, Analysis, Biosynthesis, Genetic Regulation, and Bioengineering of Production. In G. Sobero´n-Cha´vez (ed.), Biosurfactants, Microbiology Monographs 20, DOI 10.1007/978-3-642-14490-5_2, Springer-Verlag Berlin Heidelberg.

Arcamone, F., Animati, F., Bigioni, M., Capranico, G.,Caserini, C., Cipollone., A., De Cesare, M., Ettorre, A., Guano, F., Manzini, S., Monteagudo, E., Pratesi, G. 1981. Doxorubicin: anticancer antibiotics, In Medicinal Chemistry Series, vol 17, Academic Press, New York.

Assanga, S.B., Gil-Salido, A.A., Luján, L.M., Rosas-Durazo, A., Acosta-Silva, A.L., Rivera-Castañeda, E.G., Rubio-Pino, J.L., 2013. Cell growth curves for different cell lines and their relationship with biological activities. *International Journal for Biotechnology and Molecular Biology Research*, 4(4), 60-70.

Bergstrom, S., Theorell, H., Davide, H. 1946. Pyolipic Acid, a Metabolic Product of Pseudomonas-Pyocyanea, Active against Mycobacterium-Tuberculosis. *Archives of Biochemistry,* 10(1), 165–166.

Cao, X.H., Zhao, S.S., Liu, D.Y., Wang, Z., Niu, L.L., Hou, L.H., Wang, C.L. 2011. ROS-Ca2+ is associated with mitochondria permeability transition pore involved in surfactin-induced MCF-7 cells apoptosis. *Chemico-Biological Interactions*, 190(1), 16–27.

Cao, X.H., Liao, Z.Y., Wang, C.L., Yang, W.Y., Lu, M.F. 2009a. Evaluation of a lipopeptide biosurfactant from Bacillus natto TK-1 as a potential source of anti-adhesive, antimicrobial and antitumor activities. *Brazilian Journal of Microbiology :* 40(2), 373–379.

Cao, X.H., Liao, Z.Y., Wang, C.L., Cai, P., Yang, W.Y., Lu, M.F., Huang, G.W. 2009b. Purification and antitumour activity of a lipopeptide biosurfactant produced by Bacillus natto TK-1. *Biotechnology and Applied Biochemistry*, 52(Pt 2), 97–106.

Christova N, Tuleva B, Kril A, Georgieva M, Konstantinov S, Terziyski I, Nikolova B, Stoineva I. 2013. Chemical Structure and In Vitro Antitumor Activity of Rhamnolipids from Pseudomonas aeruginosa BN10. *Applied Biochemistry and Biotechnology*, 170(3), 676–689.

Chrzanowski, Ł., Ławniczak, Ł., Czaczyk, K. 2012. Why do microorganisms produce rhamnolipids? *World Journal of Microbiology and Biotechnology*, 28(2), 401–419.

Déziel, E., Lepine, F., Dennie, D., Boismenu, D., Mamer, O.A., Villemur, R. 1999. Liquid chromatography/mass spectrometry analysis of mixtures of rhamnolipids produced by Pseudomonas aeruginosa strain 57RP grown on mannitol or naphthalene. *Biochimica et Biophysica Acta - Molecular and Cell Biology of Lipids*, 1440, 244–252.

Déziel, E., Lepine, F., Milot, S., Villemur, R., 2000. Mass spectrometry monitoring of rhamnolipids from a growing culture of Pseudomonas aeruginosa strain 57RP. *Biochimica et Biophysica Acta - Molecular and Cell Biology of Lipids*, 1485(2-3), 145–152.

Duarte, C., Gudina, E.J., Lima, C.F., Rodrigues, L.R., 2014. Effects of biosurfactants on the viability and proliferation of human breast cancer cells. *AMB Express*, 4(1), p.40.

Freshney, R.I., 2010. Subculture and Cell Lines. *Culture of Animal Cells: A Basic Manual*, 1, 187–206.

Gorin, P.A.J., Spencer, J.F.T., Tulloch, A.P., 1961. Hydroxy Fatty Acid Glycosides of Sophorose From Torulopsis Magnoliae. *Canadian Journal of Chemistry*, 39(4), 846-855.

Grangemard, I., Peypoux, F., Wallach, J., Das, B.C., Caille, A., Genest, M., Dana, R.M., Ptak, M. and Bonmatin, J.M. (1997) Lipopeptides with improved properties: structure by NMR, purification by HPLC and structure-activity relationship of new isoleucylrich surfactins. *Journal of Peptide Science*, 3, 145-154.

Graves, T.G., Harr, M.W., Crawford, E.L., Willey, J.C. 2006. Stable low-level expression of p21WAFI/CIPI in A549 human bronchogenic carcinoma cell line-derived clones down-regulates E2FI mRNA and restores cell proliferation control. *Molecular Cancer* 5(1), 1-13.

Gudiña, E.J., Rangarajan, V., Sen, R., Rodrigues, L.R. 2013. Potential therapeutic applications of biosurfactants. *Trends in Pharmacological Sciences*, 34(12), pp.667–675.

Harshada, K. 2014. Biosurfactant: A Potent Antimicrobial Agent. *Journal of Microbiology and Experimentation*. 1(5), 2-5.

Holmberg, K., Jönsson, B., Kronberg, B., Lindman, B. 2003. *Surfactants and Polymers in Aqueous Solution*. 2nd edition. West Sussex: John Wiley and Sons Ltd; 562.

Hu, J., Zhang, X. and Wang, Z. 2010. Review: A Review on Progress in QSPR Studies for Surfactants. *International Journal of Molecular Sciences*, 11, 1020-1047.

Hue, N., Serani, L., Laprevote, O. 2001. Structural investigation of cyclic peptidolipids from *Bacillus subtilis* by high energy tandem mass spectrometry. *Rapid Communications in Mass Spectrometry*, 15, 203-209.

Joshi-Navare, K., Khanvilkar, P., Prabhune, A. 2013. Jatropha Oil Derived Sophorolipids: Production and Characterization as Laundry Detergent Additive. Biochemistry Research International, Volume 2013 (2013), Article ID 169797, 11 pages; (doi/10.1155/2013/169797).

Kakinuma, A., Sunino, H., Isono, M., Tamura, G., Arima, K. 1969. Determination of Fatty acid in Surfactin and Elucidation of Total Structure of Surfactin. *Agricultural and biological Chemistry*. 33(6), 973-976.

Kowall, M., Vater, J., Kluge, T., Stein, P., Ziessow, D. 1998. Separation and characterization of surfactin isoforms produced by Bacillus subtilis OKB 105. *Journal of Colloid and Interface Science*, 203, 1-8.

Lotfabad, T.B., Abassi, H., Ahmadkhaniha, R., Roostaazad, R., Masoomi, F., Zahiri, H.S., Ahmadian, G., Vali, H., Noghabi, K.A. 2010. Structural characterization of a rhamnolipid-type biosurfactant produced by Pseudomonas aeruginosa MR01: Enhancement of di-rhamnolipid proportion using gamma irradiation. *Colloids and Surfaces B: Biointerfaces*, 81(2), 397–405.

Lu, Z.J., Ren, Y.Q., Wang, G.P., Song, Q., Li, M., Jiang, S.S., Ning, T., Guan, Y.S. 2009. Biological behaviors and proteomics analysis of hybrid cell line EAhy926 and its parent cell line A549. *Journal of Experimental Clinical Cancer Research,* 28(16), 1-10.

Manivasagan P[1], Sivasankar P, Venkatesan J, Sivakumar K, Kim SK. 2014. Optimization, production and characterization of glycolipid biosurfactant from the marine actinobacterium, Streptomyces sp. MAB36, 37(5), 783-797.

Mansour, O.T., Cattoz, B., Heenan, R.K., King, S.M., Griffiths, P.C. 2015. Probing competitive interactions in quaternary formulations. *Journal of Colloid and Interface Science*, 454, 35–43.

McClements, D. 2006. Non-covalent interactions between proteins and polysaccharides. *Biotechnology Advances,* 24, 621-625.

Nitschke, M., Costa, S.G., Haddad, R., Gonc, L.A.G., Alves, N.C., Eberlin, M.N., Contiero, J. 2005. Oil wastes as unconventional substrates for rhamnolipid biosurfactant production by *Pseudomonas aeruginosa* LBI. *Biotechnology Progress,* 21(5), 1562–1566.

Ortiz, A., Teruel, J.A., Espuny, M.J., Marques, A., Manresa, A. and Aranda, F.J., 2006. Effects of dirhamnolipid on the structural properties of phosphatidylcholine membranes. *International Journal of Pharmaceutics*, 325, 99–107.

Pashley, R., Karaman, M. 2004. *Applied Colloid and Surface Chemistry*. 1st edition. West Sussex: John Wiley and Sons Ltd; 200.

Pecci, Y., Rivardo, F., Martinotti, M.G., Allegrone, G. 2010. LC/ESI-MS/MS characterisation of lipopeptide biosurfactants produced by the *Bacillus licheniformis* V9T14 strain. *Journal of Mass Spectrometry*, 45(7), 772–778.

Peypoux, F., Bonmatin, M., Labbe, H., Das, B.C., Ptak, M., Michel, G. 1991. Isolation and characterization of a new variant of surfactin, the [Val-7] surfactin. *European Journal of Biochemistry*, 202, 101-106.

Rashad, M.M., Nooman, M.U., Ali, M.M., Al-kashef, A.S., Mahmoud A.E. 2014. Production, characterization and anticancer activity of Candida bombicola sophorolipids by means of solid state fermentation of sunflower oil cake and soybean oil. *Grasas Aceites*, 65(2), 1–11.

Ribeiro, I.A.C., Faustino, C.M., Guerreiro, P.S., Frade, R.F., Bronze, M.R., Castro, M.F., Ribeiro, M.H., 2015. Development of novel sophorolipids with improved cytotoxic activity toward MDA-MB-231 breast cancer cells. *Journal of Molecular Recognition*, 28, 155–165.

Rosen, M., 1978. *Surfactants and Interfacial Phenomena*. 1st edition. Toronto: John Wiley and Sons, Inc; 322.

Scarlat, N., Dallemand, J., Monforti-Ferrario, F. and Nita, V., 2015. The role of biomass and bioenergy in a future bioeconomy: Policies and facts. *Environmental Development*, 15, 3-34.

Sousa, M., Dantas, I.T., Feitosa, F.X., Alencar, A.E.V., Soares, S.A., Melo, V.M.M., Gonçalves, L.R.B., Sant'ana, H.B. 2014. Performance of a biosurfactant produced by *Bacillus subtilis* LAMI005 on the formation of oil / biosurfactant / water emulsion: study of the phase behaviour of emulsified systems. *Brazillian Journal of Chemical Engineering*, 31(3), 613 – 623.

Stanley, F.E., Warner, A.M., Schneiderman, E., Stalcup, A.M. 2009. Rapid Determination of Surfactant Critical Micelle Concentrations Using Pressure-Driven Flow with Capillary Electrophoresis Instrumentation. *Journal of Chromatography A*, 1216(47), 8431-8434.

Tang, J.-S. Zhao, F., Gao, H., Dai, Y., Yao, Z-H., Hong, K., Li, J., Ye, W-C., Yao, X-S. 2010. Characterization and online detection of surfactin isomers based on HPLC-MSn analyses and their inhibitory effects on the overproduction of nitric oxide and the release of TNF-α and IL-6 in LPS-induced macrophages. *Marine drugs*, 8(10), 2605–2618.

Thanomsub, B., Pumeechockchai, W., Limtrakul, A., Arunrattiyakorn, P., Petchleelaha, W., Nitoda, T., Kanzaki, H. 2006. Chemical structures and biological activities of rhamnolipids produced by Pseudomonas aeruginosa B189 isolated from milk factory waste. *Bioresource Technology*, 98(5), 1149–1153.

Tonova, K., Lazarova, Z. 2008. Research review paper: Reversed micelle solvents as tools of enzyme purification and enzyme-catalyzed conversion. *Biotechnology Advances*, 26, 516–532.

Vater, J., Barbel, K., Wilde, C., Franke, P., Mehta, N., Cameotra, S.S. 2002 Matrix assisted laser desorption ionization-time of flight mass spectrometry of lipopeptide biosurfactants in whole cells and culture filtrates of *Bacillus subtilis* C-1 isolated from petroleum sludge. *Applied and Environmental Microbiology*, 68(12), 6210-6219.

Williams, S. and Brodbelt, JS. (2004) MSn characterization of protonated cyclic peptides and metal complexes. *Journal of American Society of Mass Spectrometry*, 15, 1039-1054.

Yeh, J.L., Du, S., Tortajada, A., Paulo, J., Zhang, S. 2005. Peptergents: Peptide Detergents That Improve Stability and Functionality of a Membrane Protein, Glycerol-3-phosphate Dehydrogenase. *Biochemistry*, 44, 16912-16919.

Zhao, J., Wu, Y., Alfred, A.T., Xin, X., Yang, S. 2013. Chemical structures and biological activities of rhamnolipid biosurfactants produced by pseudomonas aeruginosa M14808. *Journal of Chemical and Pharmaceutical Research*, 5(12), 177–182.

Zunino, F., Pratesi, G., Perego, P. 2001. Role of the sugar moiety in the pharmacological activity of anthracyclines: Development of a novel series of disaccharide analogs. *Biochemical Pharmacology*, 61, 933–938.

Figure legends

Figure 1 Representative chemical structures of the four selected biosurfactants: (A) mono-rhamnolipid (anionic, MW 378.41; (B) di-rhamnolipid congeners (anionic; MW 510.60); (C) Surfactin congener (zwitterionic, MW 1036.34) and (D) 1', 4"- Sophorolactone 6',6"-diacetate (non-ionic, MW 688.80)

Figure 2 ATR-FTIR spectra of 95% rhamnolipid (BS1a), 90% rhamnolipids (BS1b), surfactin (BS2) and sophorolipids (BS3).

Figure 3 Representative HPLC chromatogram of (a) surfactin (b) sophorolipids

Figure 4. Total ion chromatograms of BS1a and BS1b (A & B respectively) and corresponding mass spectra (C & D respectively)

Figure 5 Representative LC-MS spectrum of sophorolipid (BS3) sample analysed

Figure 6. Cytotoxicity of BSs on THP-1 cells after (A). 24 hr (B). 48 hr (C). 72 hr (n = 3, ± SD)

Figure 7. Plots showing the cytotoxicity of BS3 on MCF-7 cells after (A). 24 hr (B). 48 hr (C). 72 hr (n = 4, ± SD).

FIGURES

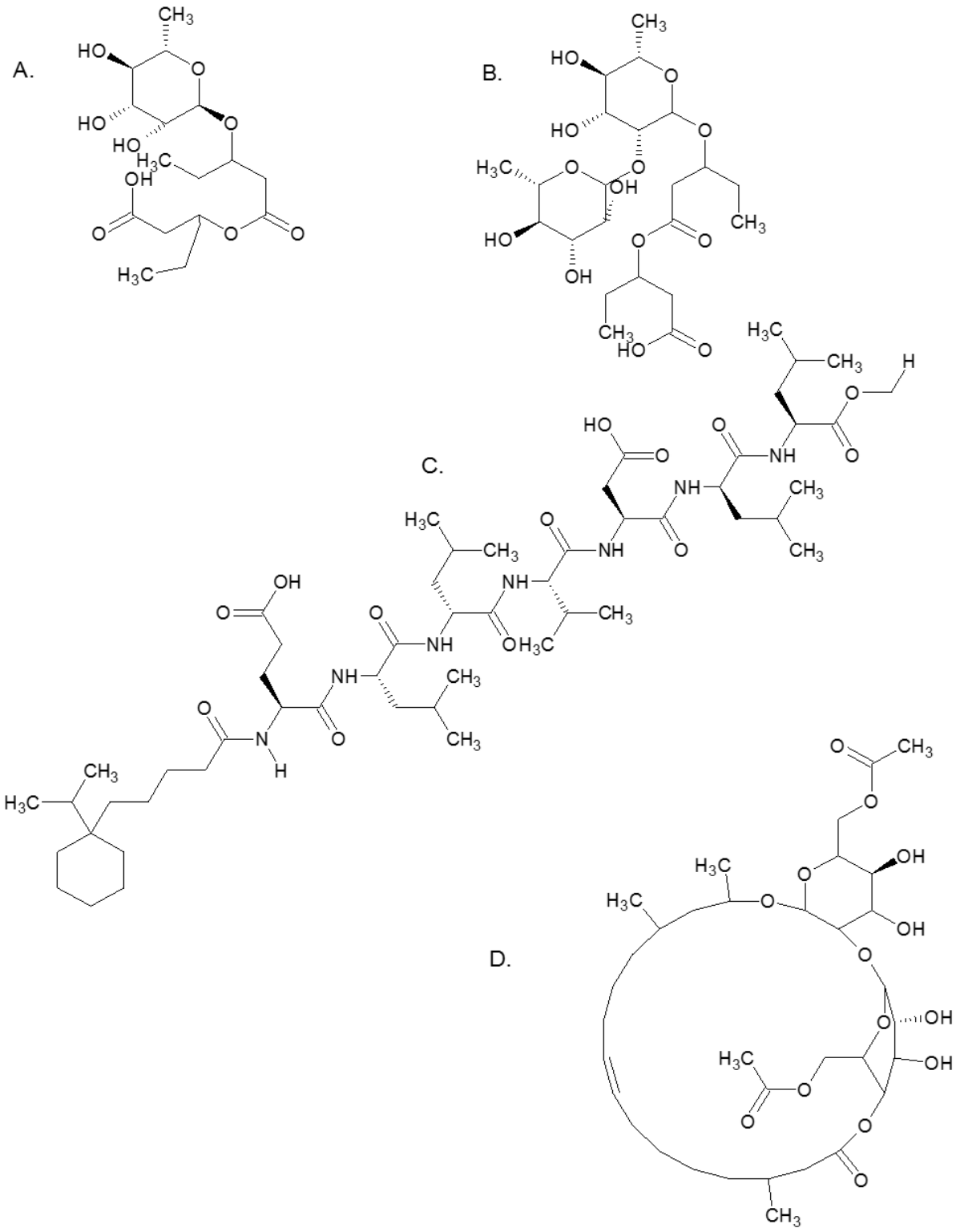

Figure 1

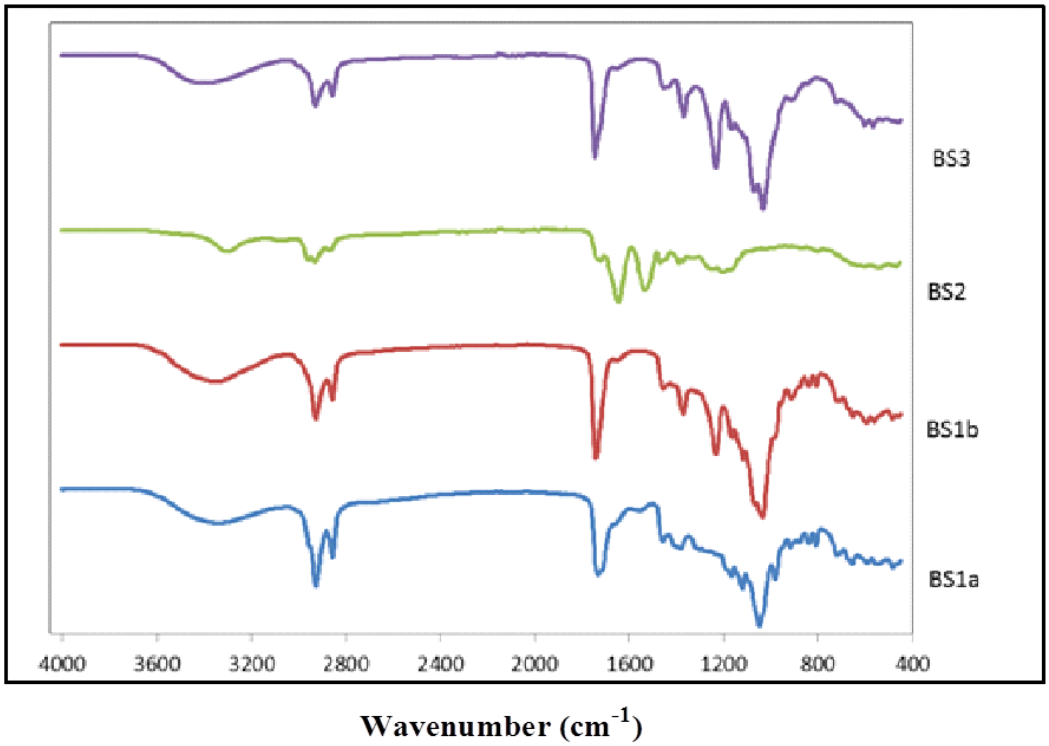
BS3
BS2
BS1b
BS1a
4000
3600
3200
2800
2400
2000
1600
1200
800
400
Wavenumber (cm-1)

Figure 2

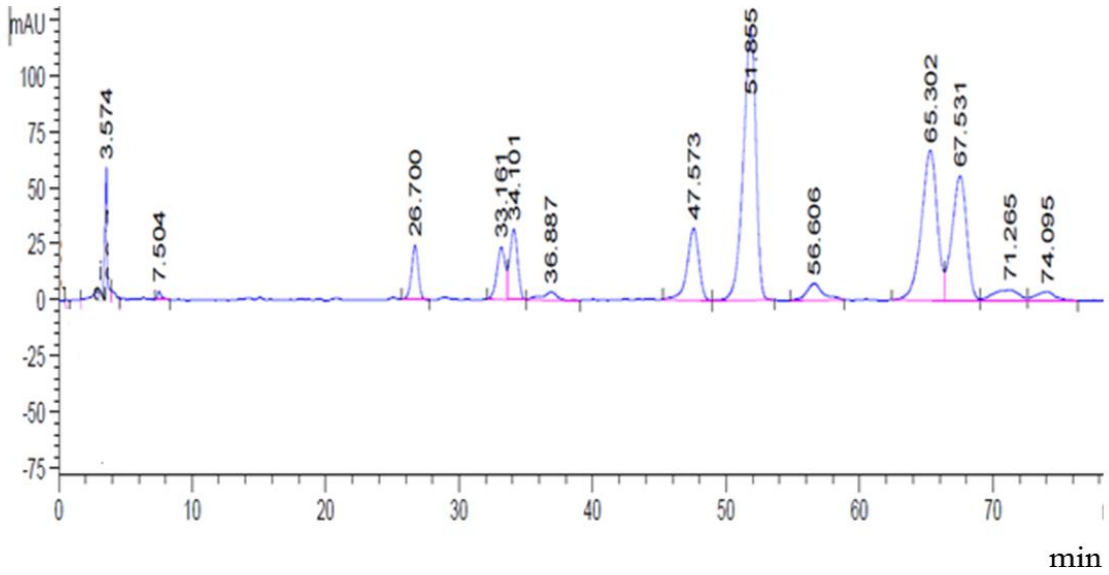
mAU
100
75
50
25
0
-25
-50
-75
3.574
7.504
26.700
33.161
34.101
36.887
47.573
51.855
56.606
65.302
67.531
71.265
74.095
0
10
20
30
40
50
60
70
min

(a)

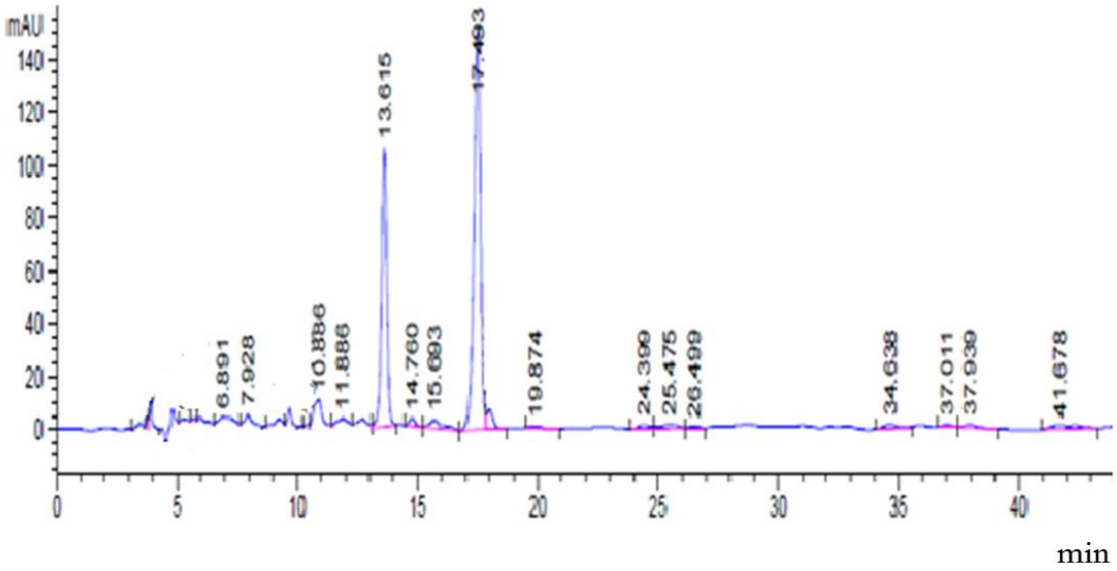
mAU
140
120
100
80
60
40
20
0
6.891
7.928
10.886
11.886
13.615
14.760
15.693
17.493
19.874
24.399
25.475
26.499
34.638
37.011
37.939
41.678
0
5
10
15
20
25
30
35
40
min

(b)

Figure 3

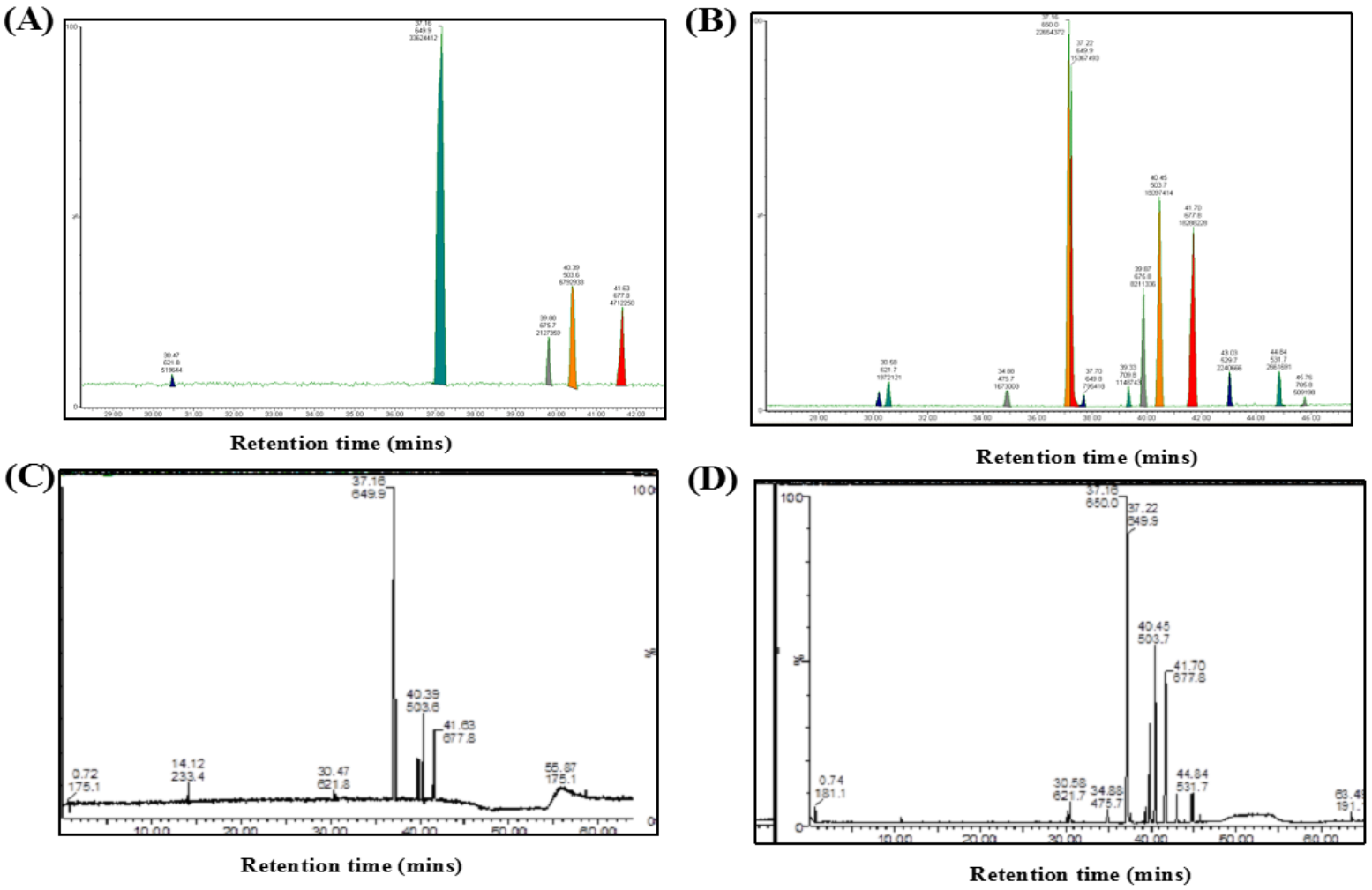
(A)
Retention time (mins)
(B)
Retention time (mins)
(C)
37.16
649.9
40.39
503.6
41.63
677.8
0.72
175.1
14.12
233.4
30.47
621.8
55.87
175.1
Retention time (mins)
(D)
37.16
650.0
37.22
649.9
40.45
503.7
41.70
677.8
0.74
181.1
30.58
621.7
34.88
475.7
44.84
531.7
Retention time (mins)

Figure 4

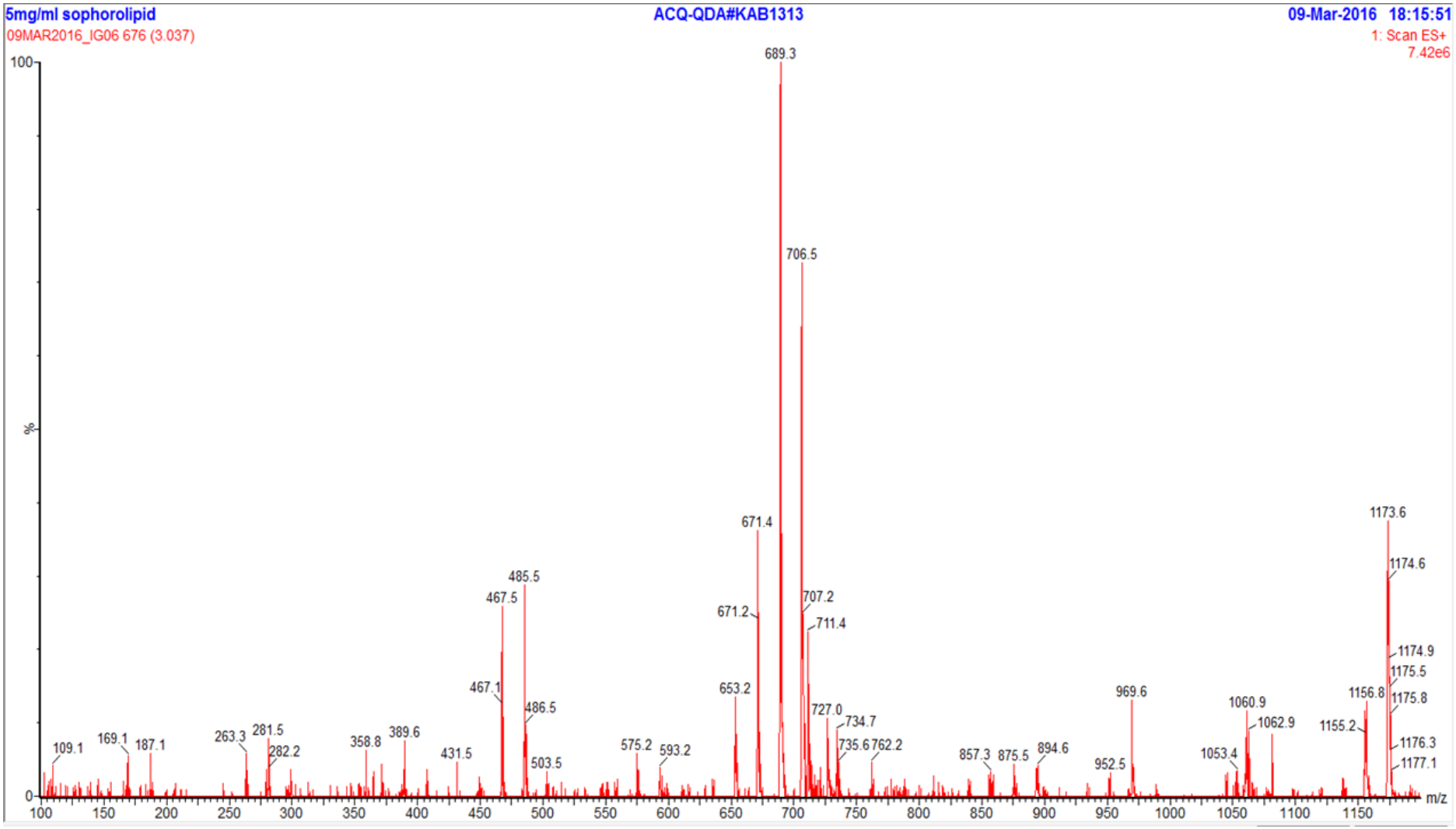
5mg/ml sophorolipid
09MAR2016_IG06 676 (3.037)
ACQ-QDA#KAB1313
09-Mar-2016 18:15:51
1: Scan ES+
7.42e6
100
%
0
m/z
689.3
706.5
671.4
671.2
485.5
467.5
707.2
711.4
467.1
486.5
653.2
727.0
734.7
735.6
762.2
503.5
575.2
593.2
431.5
358.8
389.6
263.3
281.5
282.2
109.1
169.1
187.1
857.3
875.5
894.6
952.5
969.6
1053.4
1060.9
1062.9
1155.2
1156.8
1173.6
1174.6
1174.9
1175.5
1175.8
1176.3
1177.1
100
150
200
250
300
350
400
450
500
550
600
650
700
750
800
850
900
950
1000
1050
1100
1150

Figure 5

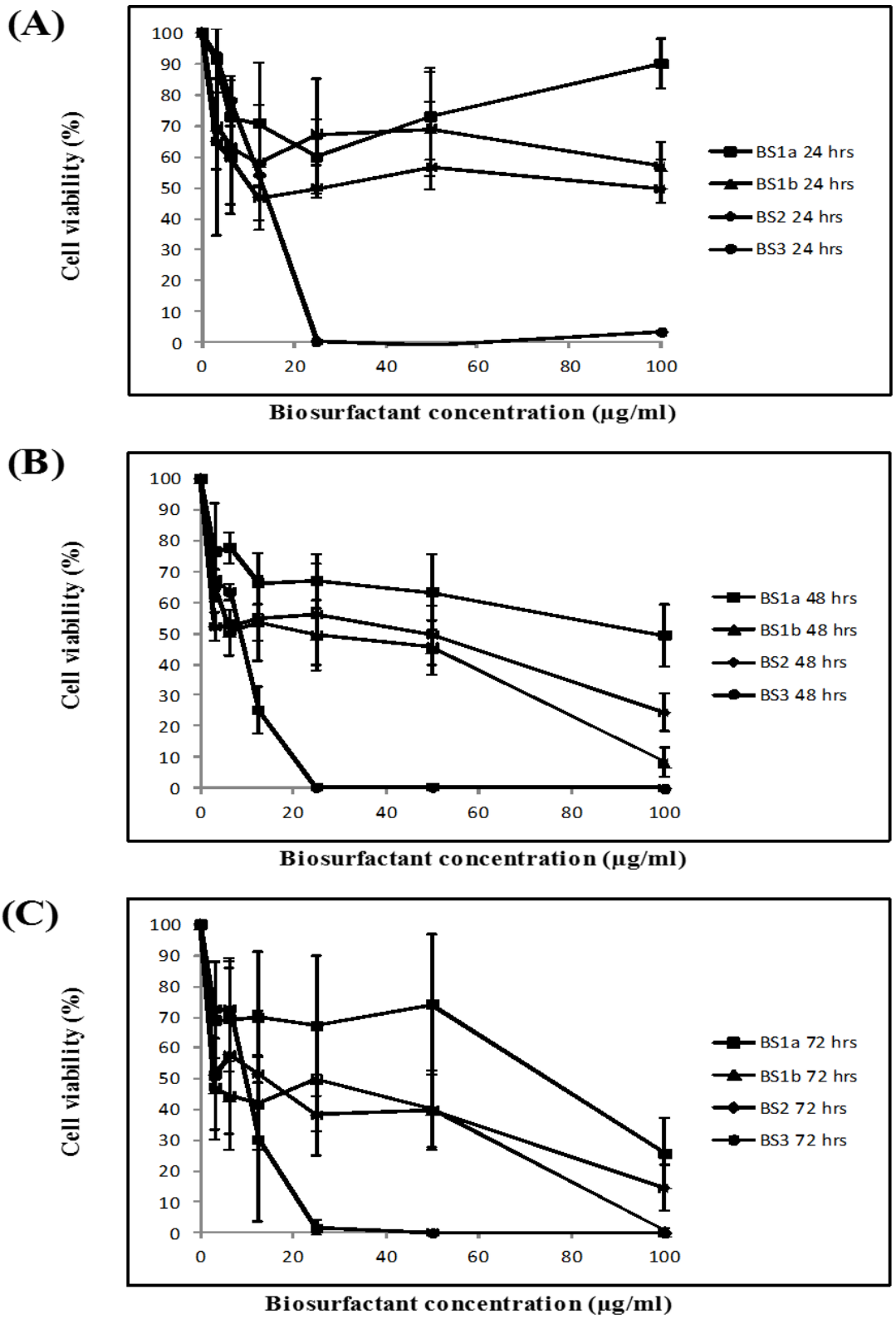
(A)
Cell viability (%)
100
90
80
70
60
50
40
30
20
10
0
0
20
40
60
80
100
Biosurfactant concentration (µg/ml)
BS1a 24 hrs
BS1b 24 hrs
BS2 24 hrs
BS3 24 hrs
(B)
Cell viability (%)
Biosurfactant concentration (µg/ml)
BS1a 48 hrs
BS1b 48 hrs
BS2 48 hrs
BS3 48 hrs
(C)
Cell viability (%)
Biosurfactant concentration (µg/ml)
BS1a 72 hrs
BS1b 72 hrs
BS2 72 hrs
BS3 72 hrs

Figure 6

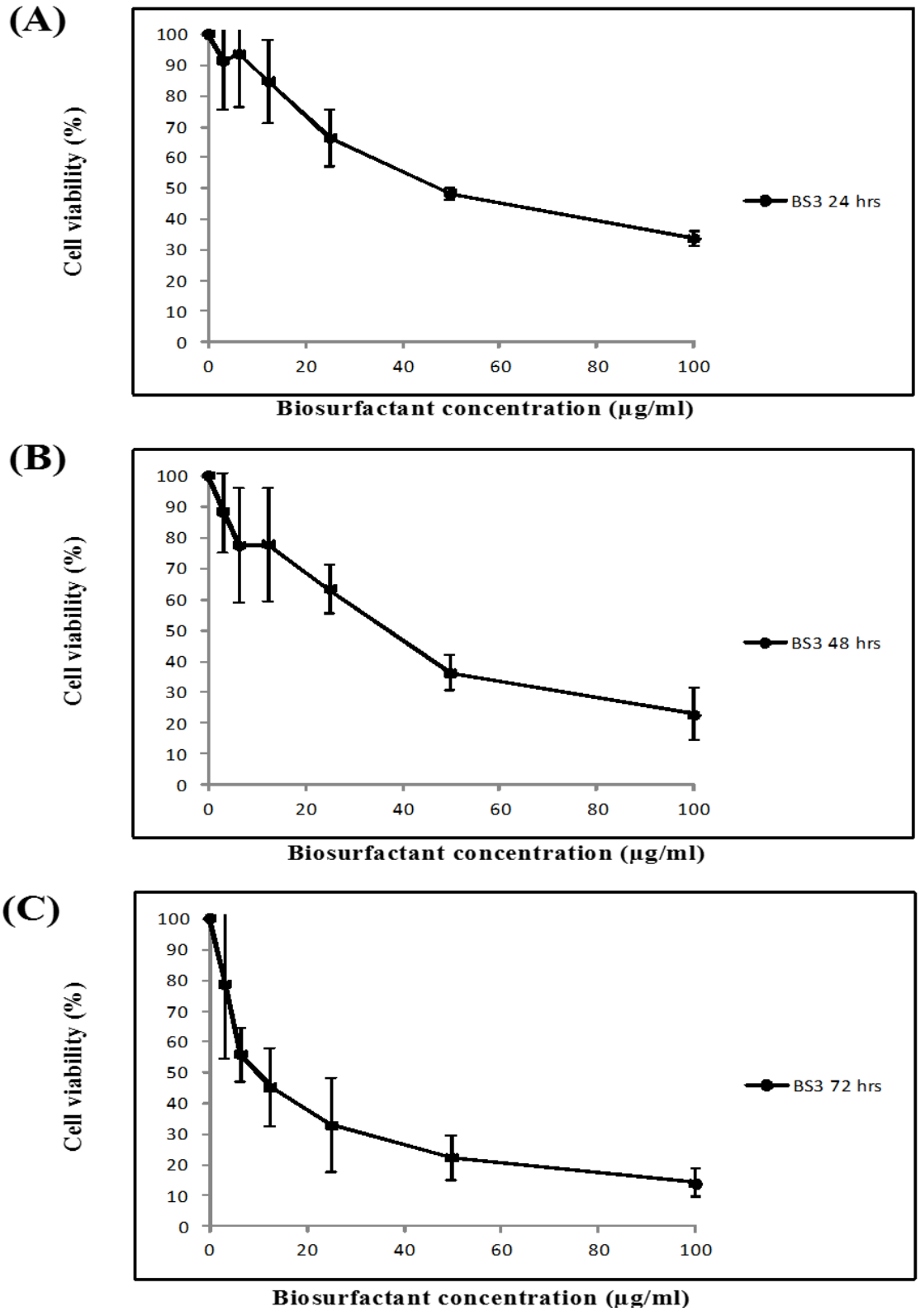
(A)
Cell viability (%)
100
90
80
70
60
50
40
30
20
10
0
0
20
40
60
80
100
BS3 24 hrs
Biosurfactant concentration (µg/ml)
(B)
Cell viability (%)
BS3 48 hrs
Biosurfactant concentration (µg/ml)
(C)
Cell viability (%)
BS3 72 hrs
Biosurfactant concentration (µg/ml)

Figure 7